ASPS Conference Proceedings 1: 857-865 (2022)

Proceedings of

12th Structural Engineering Convention-An International Event (SEC 2022)

Available at https://asps-journals.com/index.php/acp

Seismic Analysis of Sagging Elasto-flexible Cable using Placement Model

Pankaj Kumar [1, *], Sanjay Tiwari [2], S.K. Jain [2], Ritu Raj [3]

[1] Department of Civil Engineering, Assistant Professor, Madhav Institute of Technology and Science Gwalior 474005, India
[2] Department of Civil Engineering, Professor, Madhav Institute of Technology and Science Gwalior 474005, India
[3] Department of Civil Engineering, Assistant Professor, Delhi Technological University, Delhi 110042, India

Paper ID - 060401

Abstract

Weightless sagging elasto-flexible cables lack unique natural state. However, heavy cables are assumed their natural state under their self-weight for predicting their static and dynamic response. In most of the existing literatures the nodal coordinates or placements are generally defined in reference to the chosen Cartesian coordinate system for the discrete formulation called here Placement Model. In this paper, Placement Model is applied to predict the seismic response of weightless sagging cables. The cable is fixed at their both the ends and two masses are attached in its intermediate points leading to a 2-node 4-DOF system. The dynamic response of the cable node is investigated by applying two different seismic excitations in three different conditions as only horizontal excitation, only vertical excitation and both horizontal and vertical excitation act simultaneously. El-Centro and Loma Preta Seismic excitation is applied to predict the seismic response of the cables.

Keywords: Sagging elastic cable, seismic response, earthquake, placement model, symmetric vibration, anti-symmetric vibration

1. Introduction

The cables are used in diverse areas of structural engineering. It is well-known that elasto-flexible sagging cables lack unique natural reference configuration in their passive state. However, it is assumed that the equilibrium configuration under its self-weight as the reference configuration. Now these days quite sophisticated analytical and computational techniques have been used for obtaining the static and dynamic response of cables. The behaviour of cables shows inherent nonlinearity. In addition to this, the presence of self-weight renders the response of the cable to another type of nonlinearity. Linear modal frequencies of single sagging cables depend upon their elasto-geometrical parameters [1, 2]. Most of the investigations on cables are considering its self-weight and under points load. Under self-weight the shape of the cable is found catenary [3, 4]. A spatial two- node catenary cable element with derived tangent stiffness matrix is proposed for conducting nonlinear seismic analysis of cable structures under self-weight and concentrated loads [5]. Such a popular approach using elastic and geometric stiffness matrices for dynamic analysis for nonlinear cables has been criticized [6]. Phenomenon of internal resonances and subharmonic resonances has been predicted for these nonlinear structures [7].

The main point of departure in the approach by the authors is the assumed weightlessness of the cables and the lack of their unique natural configuration. Static and dynamic response of a single weightless elasto-flexible sagging planer cable carrying lumped nodal masses and applied nodal loads leading to a 2-node 4-DOF cable system has earlier been investigated. Rate-type constitutive equations and third order differential equations of motion of have been derived. The dynamic response of such structures to harmonic nodal force is determined for different sustained nodal forces, axial elastic stiffness and sag/span ratios. Sub harmonic resonances, jump and beat phenomenon are predicted for elastic and inextensible cables [8]. In another approach the incremental equation of motion involving tangent stiffness matrix employed is equivalent to the third order equation of motion proposed [5].

In the discrete formulation, the nodal coordinates or placements are generally defined in reference to the chosen Cartesian coordinate system and this approach is called Placement Model. In Placement Models, the nodal deformed placements constitute the primary kinematic variables in the equation of motion.

In this paper we have adopted the Placement Model to develop the stiffness matrix of the 2-node 4-DOF cable system and further dynamic analysis. The constitutive equations and equations of motion earlier developed [8] is applied here for seismic analysis of a particular sagging planer cable structure. Also, the Placement Model developed is compared with the earlier developed Force Model [9].

As required by the equation of motion, the time-derivative of the two well-known seismic excitations is obtained. Dynamic response is investigated under horizontal and vertical seismic excitations applied separately as well as

*Corresponding author. Tel: +919968270408; E-mail address: pankaj437@gmail.com

Proceedings of the 12th Structural Engineering Convention (SEC 2022), NCDMM, MNIT Jaipur, India| 19-22 December, 2022

Published online: December 19, 2022
doi:10.38208/acp.v1.594

simultaneously. In this paper, it is assumed that the vertical component of the ground acceleration is two-third of the horizontal component of the ground acceleration.

For seismic analysis of Indiano Bridge, finite element analysis is used and the material is assumed as linear elastic. High amplitude longitudinal vibrations is observed [10, 11]. In this paper the material is assumed as linear elastic and the damping is assumed as instantaneously classically damped i.e. the damping matrix is a function of stiffness and mass matrices.

Seismic analysis of transmission line system under El Centro ground excitation on are investigated with different boundary conditions. The vertical displacement of middle span of the transmission line is obtained maximum due to anti-symmetric modes of the transmission lines (Tian L. and Xia G. 2016). In this paper the assumed cable system is investigated under both El Centro and Loma Prieta ground excitations.

2. Equation of Motion and constitutive relation

The placement model is derived here for the 2-node 4-DOF planar sagging cable tied at both the ends (Fig. 1). Undeformed segment lengths of the cable are known in addition to the coordinates of the tied end D in reference to the coordinate system with origin at the end A.

Assuming the nodal placements (y_i) in the deformed state of the cable as y_i, the axial extensions as Δ_r and tensile forces in its segments as T_r. The segment tensile forces are obtained as

$$T_1 = \frac{EA\Delta_1}{S_1} \qquad T_2 = \frac{EA\Delta_2}{S_2} \qquad T_3 = \frac{EA\Delta_3}{S_3} \tag{1}$$

Also, the axial elastic extension in the cable segments are expressed as

$$\begin{aligned} \Delta_1 &= \sqrt{(y_1^2 + y_2^2)} - S_1; \\ \Delta_2 &= \sqrt{\{(y_3 - y_1)^2 - (y_4 - y_2)^2\}} - S_2; \\ \Delta_3 &= \sqrt{\{(L - y_3)^2 - (H - y_4)^2\}} - S_3 \end{aligned} \tag{2}$$

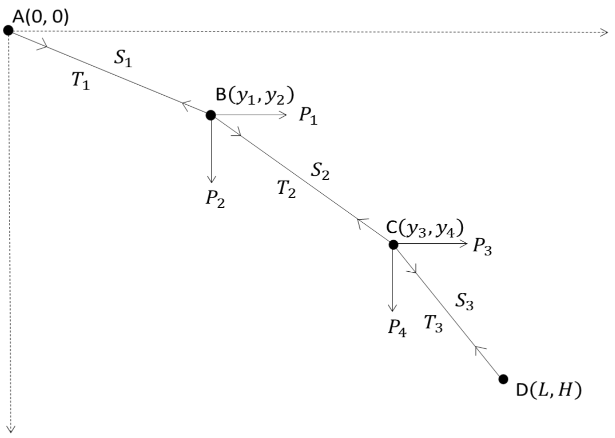

Fig. 1 Two-node four-DOF cable tied at both ends

The nodal equilibrium conditions are used to obtained the nodal loads (P_i) in terms of the deformed state nodal placements (y_i) as

$$\begin{aligned} P_1 &= T_1\left(\frac{y_1}{L_1}\right) - T_2\left(\frac{y_3 - y_1}{L_2}\right); \\ P_2 &= T_1\left(\frac{y_2}{L_1}\right) - T_2\left(\frac{y_4 - y_2}{L_2}\right); \\ P_3 &= T_2\left(\frac{y_3 - y_1}{L_2}\right) - T_3\left(\frac{L - y_3}{L_3}\right); \\ P_4 &= T_2\left(\frac{y_4 - y_2}{L_2}\right) - T_3\left(\frac{H - y_4}{L_3}\right); \end{aligned} \tag{3}$$

The nodal elastic displacements (u_i) can also be represented as the components of the axial elastic extensions (Δ_r) along the coordinate axes and are expressed as

$$\begin{aligned} u_1 &= \Delta_1 \frac{y_1}{L_1}; \qquad & u_2 &= \Delta_1 \frac{y_2}{L_1}; \\ u_3 &= -\Delta_3 \frac{(L - y_3)}{L_3}; \qquad & u_4 &= -\Delta_3 \frac{(H - y_4)}{L_3}; \end{aligned} \tag{4}$$

Substituting of expressions for tensile forces in above equations in terms of nodal placements, the following nodal load-placement relations $\{P = P(y)\}$ are obtained as

$$\begin{aligned} P_1 &= EA\left[\left\{\frac{(y_3 - y_1)}{L_2} - \frac{y_1}{L_1}\right\} - \left\{\frac{(y_3 - y_1)}{S_2} - \frac{y_1}{S_1}\right\}\right] \\ P_2 &= EA\left[\left\{\frac{(y_4 - y_2)}{L_2} - \frac{y_2}{L_1}\right\} - \left\{\frac{(y_4 - y_2)}{S_2} - \frac{y_2}{S_1}\right\}\right] \\ P_3 &= EA\left[\left\{\frac{(L - y_3)}{L_3} - \frac{(y_3 - y_1)}{L_2}\right\} - \left\{\frac{(L - y_3)}{S_3} - \frac{(y_3 - y_1)}{S_2}\right\}\right] \\ P_4 &= EA\left[\left\{\frac{(H - y_4)}{L_3} - \frac{(y_4 - y_2)}{L_2}\right\} - \left\{\frac{(H - y_4)}{S_3} - \frac{(y_4 - y_2)}{S_2}\right\}\right] \end{aligned} \tag{5}$$

The incremental constitutive equation is established as $dP_i = K_{ij}\, dy_j$, where the tangent stiffness matrix coefficients as $K_{ij} = \partial P_i / \partial y_j$. The rate-type constitutive equation relating these internal nodal forces P_i and the nodal coordinates y_j is stated as

$$\dot{P}_i = K_{ij}\, \dot{y}_j \tag{6}$$

Consider a two-node four-DOF weightless planer sagging elasto-flexible cable with attached masses as shown in Fig. 2. Let y_i denote the deformed nodal coordinates of the cable carrying sustained nodal loads.

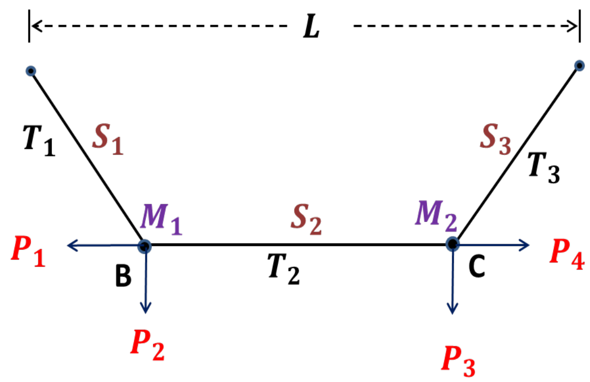

Fig. 2 Two-node four-DOF symmetrical system

The following third order coupled nonlinear differential equations of motion are derived for such cables carrying lumped masses M_{ij}.

$$M_{ij}\dddot{y}_i + C_{ij}\ddot{y}_i + K_{ij}\dot{y}_i = \dot{F}_i(t) \tag{7}$$

The internal resistive nodal forces P_i are obtained as

$$P_i = F_i(t) - M_{ij}\ddot{y}_i - C_{ij}\dot{y}_i \quad (8)$$

Here, the nonlinear cable structure is assumed to be instantaneously classically damped with the instantaneous damping matrix C_{ij} being determined as

$$C_{ij} = a_0 M_{ij} + a_1 K_{ij} \quad (9)$$

3. Structural and loading details

The seismic analysis of a planar cable net has been investigated earlier by Thai and Kim (2011). For investigation in this paper a particular single planar sagging cable is chosen from that cable net by idealization as shown in Fig. 2. The structural details are given below:

$E = 82737$ MPa; $L = 91.44$ m; $A = 146.45\ mm^2$; $H = 0$
$F_0 = (0, 17.793, 0, 17.793)$ kN

Two equal masses (M = 4380 kg) are attached at the two nodes. Self-weight of the cable is ignored. Using Newoton-Raphson Method following cable configuration and segment tension are obtained:

$y_1 = 30.41$; $y_2 = 9.87$ m; $y_3 = 61.02$ m; $y_4 = 9.87$ m
$T_1 = 57.62$ kN; $T_2 = 54.80$ kN; $T_3 = 57.62$ kN

The linear modal frequencies given by eigenvalues of the matrix $M_{ij}^{-1}K_{ij}$ are obtained as $\omega_{n1} = 1.07$ rad/s; $\omega_{n2} = 2.47$ rad/s; $\omega_{n3} = 9.32$ rad/s; $\omega_{n4} = 16.20$ rad/s.

In the presence of seismic excitation, the nodal force vector is obtained as

$$F_i(t) = F_{0i} + E_i(t) \quad (10)$$

Where $E_i(t)$ represents the applied time-dependent seismic forces. It is assumed that the dynamic forces introduced by the earthquakes and acting on the nodal masses are lying in the plane of the cable. Also, these forces depend upon the horizontal and vertical components of the seismic acceleration. In the case when only horizontal seismic forces are considered

$$E_h(t) = (-M_1\ddot{y}_h, 0, -M_2\ddot{y}_h, 0) \quad (11)$$

Similarly, when only vertical seismic forces are acting

$$E_v(t) = (0, -M_1\ddot{y}_v, 0, -M_2\ddot{y}_v) \quad (12)$$

In fact, the horizontal and the vertical components of the seismic forces act simultaneously. In this paper, it is assumed that the vertical component of the ground acceleration is two- third of the horizontal component of the ground acceleration with same frequency content. As the equation of motion is third order differential equation, rate of loading vector is also needed. In the case of horizontal and vertical seismic accelerations, the loading rate vectors are represented as

$$\begin{aligned} \dot{E}_h(t) &= (-M_1\dddot{y}_h, 0, -M_2\dddot{y}_h, 0) \\ \dot{E}_v(t) &= (0, -M_1\dddot{y}_v, 0, -M_2\dddot{y}_v) \end{aligned} \quad (13)$$

Here, $\dddot{y}_h$ and $\dddot{y}_v$ are the rates of change of horizontal and vertical components of ground acceleration respectively. Here, $\dddot{y}_h$ and $\dddot{y}_v$ are determined from the available ground acceleration components $\ddot{y}_h$ and $\ddot{y}_v$ respectively as

$$\begin{aligned} \dddot{y}_{h\left(t_i+\frac{\Delta t}{2}\right)} &= \frac{\ddot{y}_{h(t_i+\Delta t)} - \ddot{y}_{h(t_i-\Delta t)}}{2\Delta t} \\ \dddot{y}_{v\left(t_i+\frac{\Delta t}{2}\right)} &= \frac{\ddot{y}_{v(t_i+\Delta t)} - \ddot{y}_{v(t_i-\Delta t)}}{2\Delta t} \end{aligned} \quad (14)$$

From the available records for the El Centro Southern California, US earthquake (1940), the horizontal ground acceleration components and the deduced rate of acceleration normalized with respect to acceleration due to gravity is plotted in Fig. 3(a) and Fig. 3(b) respectively. As the seismic response of structures also depend upon their modal frequencies as well as the frequency content of the applied excitation. For better understanding and easy interpretation of dynamic response, Fast Fourier Transform (FFT) of the same ground acceleration as well as the rate of ground acceleration is presented in Fig. 3(c) and 3(d).

Similar characteristics of the Loma Prieta, California's Central Coas, US earthquake (1989) are presented in Fig. 4(a), 4(b), 4(c) and 4(d) respectively. It is observed that the peak ground acceleration (PGA) of the El Centro and the Loma Prieta earthquakes are 0.3163g and 0.5235g respectively with 'g' as acceleration due to gravity. It is also observed that the dominant frequency ranges for the El Centro and the Loma Prieta seismic accelerations lies between 5 to 45 rad/s and 4 to 25 rad/s respectively. The corresponding frequency ranges for of the dominant rate of seismic accelerations are 13 to 42 rad/s^2 and 17 to 52 rad/s^2.

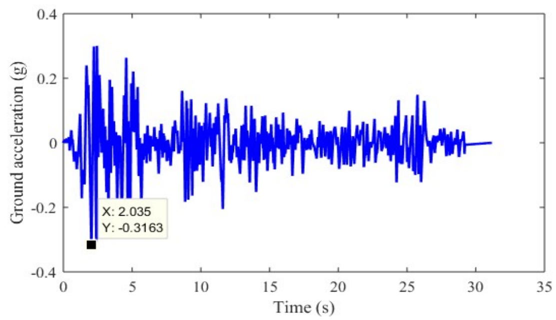

Fig. 3(a) Ground acceleration (El Centro)

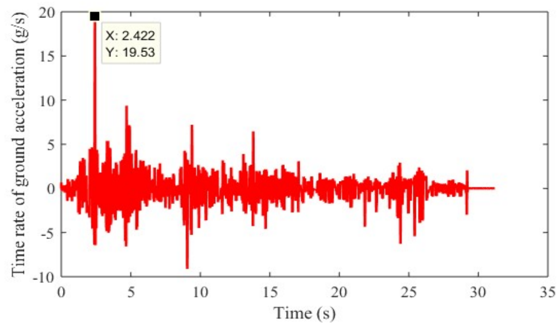

Fig. 3(b) Time rate of ground acceleration (El Centro)

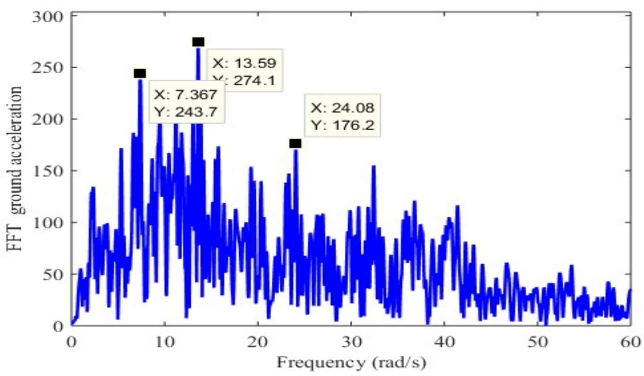

Fig. 3(c) FFT of ground acceleration (El Centro)

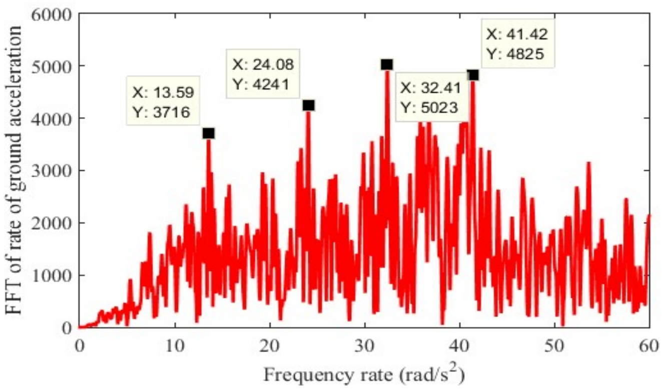

Fig. 3(d) FFT of rate of ground acceleration (El Centro)

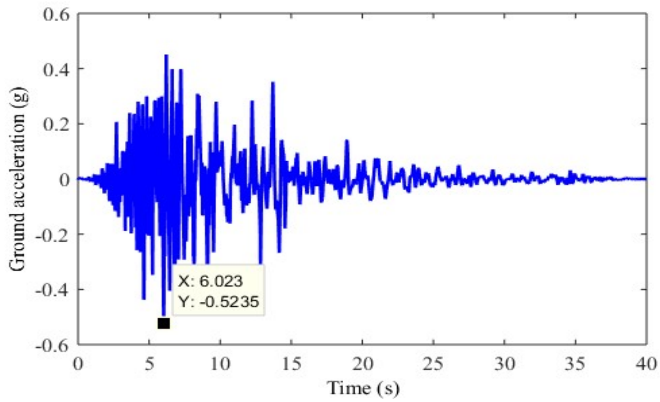

Fig. 4(a) Ground acceleration (Loma Prieta)

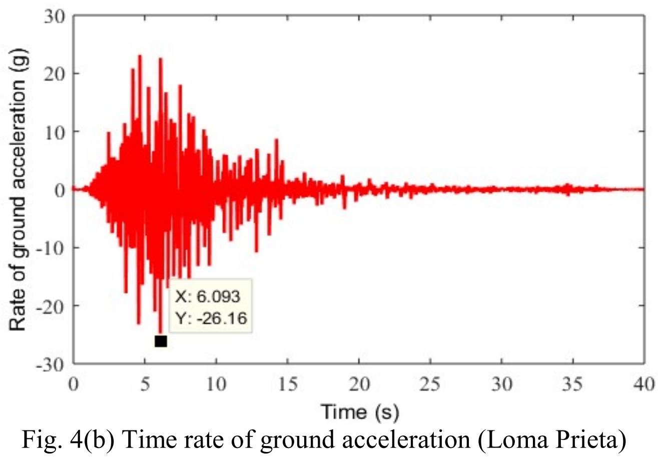

Fig. 4(b) Time rate of ground acceleration (Loma Prieta)

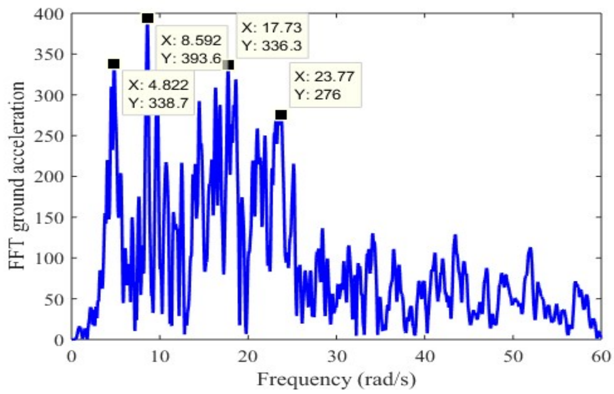

Fig. 4(c) FFT of ground acceleration (Loma Prieta)

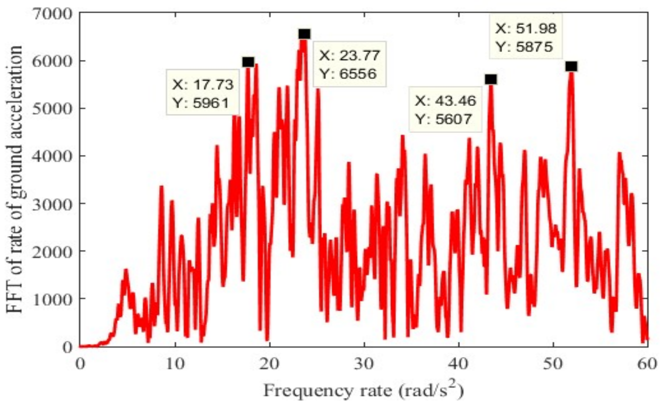

Fig. 4(d) FFT of rate of ground acceleration (Loma Prieta)

4. Predicted seismic response: El Centro Earthquake

The dynamic response of the chosen cable structure is investigated with following three cases of ground motion as (i) Horizontal excitation (ii) Vertical excitation and (iii) Combination of both horizontal and vertical excitation.

4.1 Only horizontal excitation is applied

When only horizontal seismic force is applied to the cable structure, then peak vertical nodal response is about twice than the peak horizontal nodal response as shown in the Fig. 5(a) and 5(b). Also, the vertical nodal responses of both nodes are in opposite phase but same magnitude, whereas the horizontal response of both the nodes are in same phase and same magnitude.

Tension increment is plotted for all three cable segments. It is very interesting to note that, the predicted tension increment in the inclined cables are much large than that of horizontal cable segment as shown in Fig. 6(a) and Fig. 6(b) respectively. Also, the tension increment waveform for inclined cable shows opposite phase with same magnitude. Here negative sign does not mean compressive axial force, but the decrease in the axial tensile force.

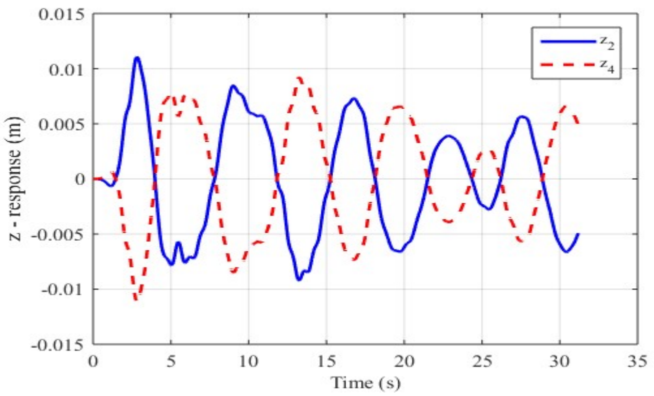

Fig. 5(a) Vertical nodal response

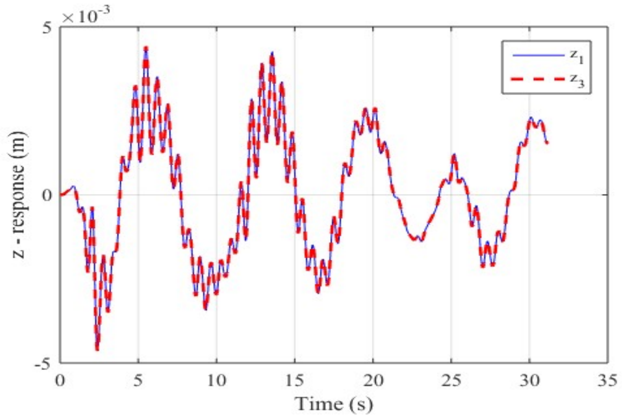

Fig. 5(b) Horizontal nodal response

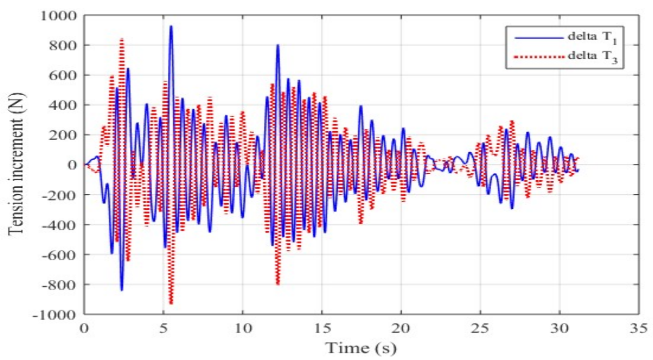

Fig. 6(a) Tension increment of inclined cable segments

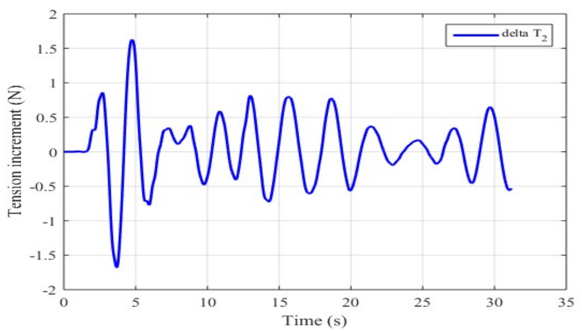

Fig. 6(b) Tension increment of horizontal cable segments

4.2 Only vertical excitation is applied

In case when only vertical seismic excitation is applied to the system, the peak vertical nodal response of none 2 is about ten times the peak horizontal nodal response as shown in the Fig. 7(a) and 7(b). Also, the vertical nodal response of node 1 is interestingly much lower than the vertical nodal response of node 2. The horizontal response of both the nodes are same in magnitude but with opposite phase.

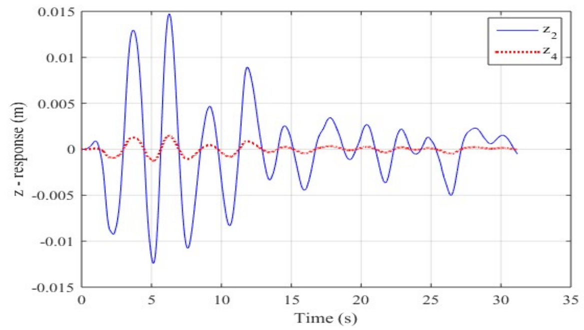

Fig. 7(a) Vertical nodal response

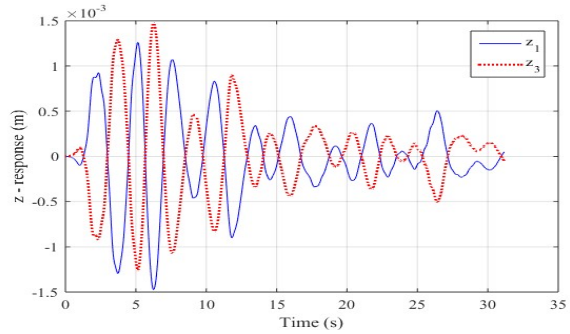

Fig. 7(b) Horizontal nodal response

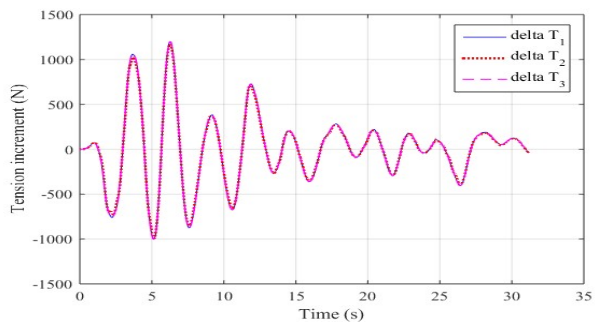

Fig. 8 Tension increment in all cable segments

Tension increment is plotted for each three cable segments in Fig. 8. The predicted tension increments in all three cable segments for vertical seismic excitation are same.

4.3 Both horizontal and vertical excitation is applied

When both vertical and horizontal seismic excitation is applied simultaneous to the cable structures, both the peak horizontal and vertical nodal response is observed to be higher compared to earlier cases when only horizontal or only vertical excitation is applied respectively. Also the nature of predicted waveform is different in this case as shown in in Fig. 9(a) and 9(b).

The predicted tension increment in all three cable segments of each three cable segments are shown in the Fig. 10. The predicted tension response shows that, the increment in tension of inclined segment is slightly more than the horizontal segment. It is interesting to note that, the pattern of tension increment is similar for all three segments.

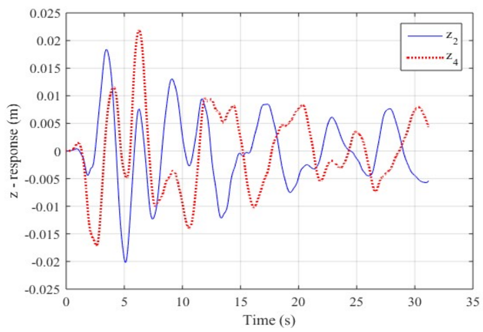

Fig. 9(a) Vertical nodal response

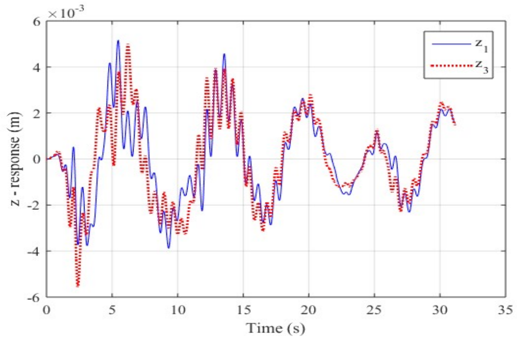

Fig. 9(b) Horizontal nodal response

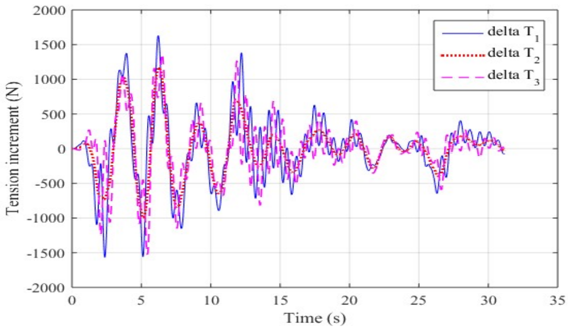

Fig. 10 Tension increment in all cable segments

5. Predicted seismic response: Loma Preita Earthquake

5.1. Only horizontal excitation is applied

In this case the Loma Preita seismic excitation is applied in all three cases. When only horizontal seismic force is applied to the cable structure, the vertical nodal response is of both the nodes shows similar response but out of phase as shown in the Fig. 11(a). Whereas the horizontal nodal response of both the nodes are exactly similar in nature as shown in Fig. 11(b).

The predicted tension response of inclined cable segments shows much higher increment than horizontal cable segments. The tension increments of both the inclined segments are similar in magnitudes but opposite in phase as shown in Fig. 12(a). Almost no change in the tension of horizontal segment is occurred as shown in Fig. 12(b).

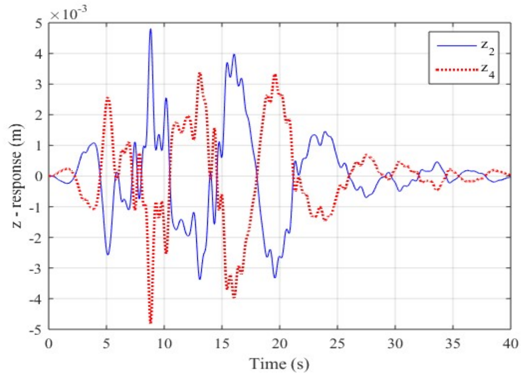

Fig. 11(a) Vertical nodal response

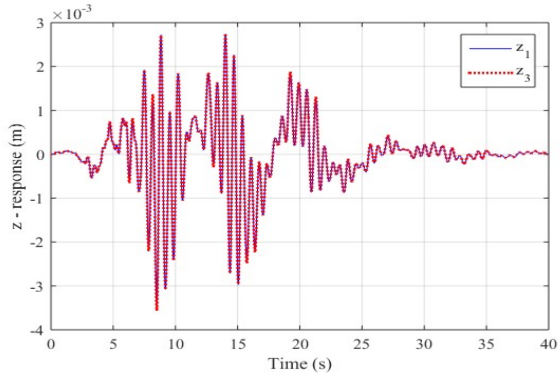

Fig. 11(b) Horizontal nodal response

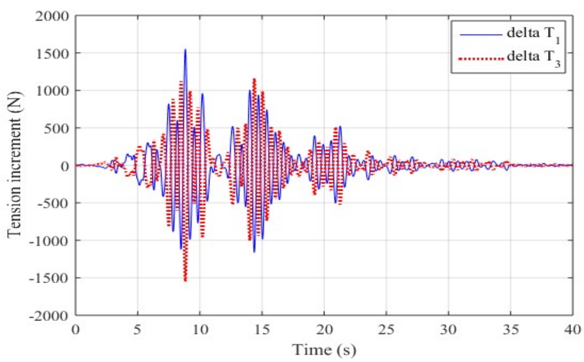

Fig. 12(a) Tension increment of inclined cable segments

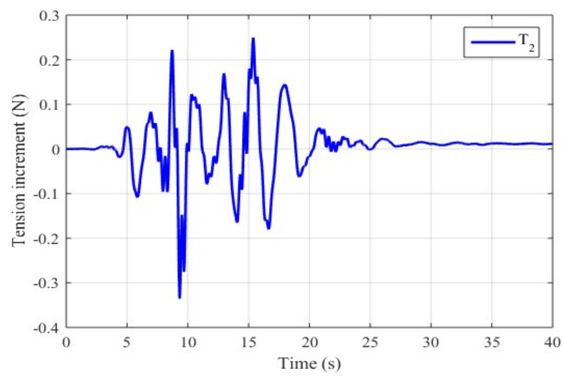

Fig. 12(b) Tension increment of horizontal cable segments

5.2. Only vertical excitation is applied

When only vertical Loma Preita seismic excitation is applied to the cable structure, the vertical nodal response is of both the nodes as shown in the Fig. 13(a) have similar response with same phase. In other words the vertical response of both the nodes coincides with each other as shown in the figure. However the horizontal nodal responses of both the nodes are similar in magnitudes but having opposite phase as shown in Fig. 13(b).

The predicted tension of all the three cable segments shows almost similar response as shown in Fig. 14. However at few time instant the tension response of horizontal cable segment differ slightly with inclined cable tension response. Also the magnitude of tension increment in this case is about half of that of previous case when only horizontal seismic force is applied.

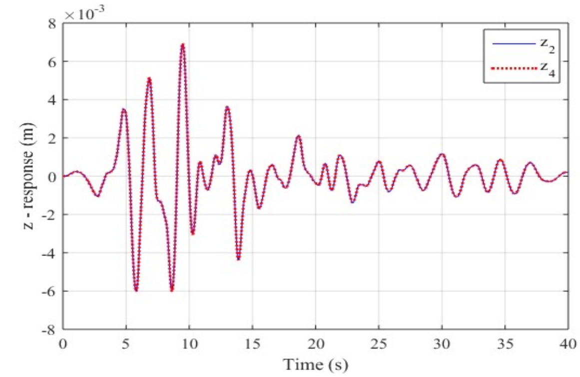

Fig. 13(a) Vertical nodal response

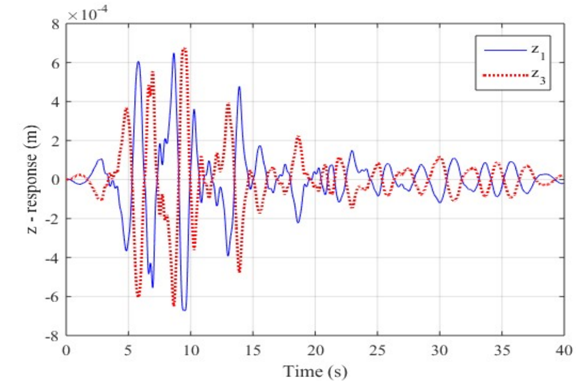

Fig. 13(b) Horizontal nodal response

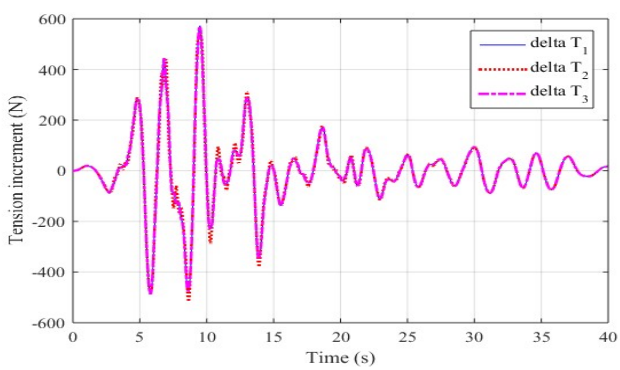

Fig. 14 Tension increment in all cable segments

5.3. Both horizontal and vertical excitation is applied

When both vertical and horizontal seismic excitation is applied simultaneous to the cable structures, the vertical nodal response shows similar phase in first last few seconds while opposite phase in middle of the excitation. However the magnitude of vertical response of both the nodes changes relatively with time passes as shown in in Fig. 15(a). The horizontal nodal response shows about half the magnitude of corresponding vertical nodal response. Also, both nodes show relatively similar horizontal response as shown in Fig. 15(b).

The predicted tension increment in inclined cable segments are about double that of horizontal cable segments are shown in the Fig. 16(a) and Fig. 16(b) respectively.

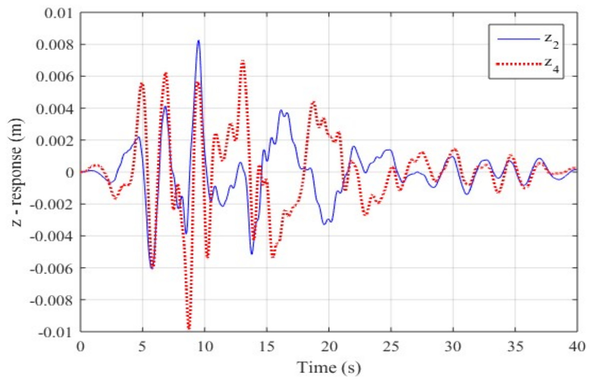

Fig. 15(a) Vertical nodal response

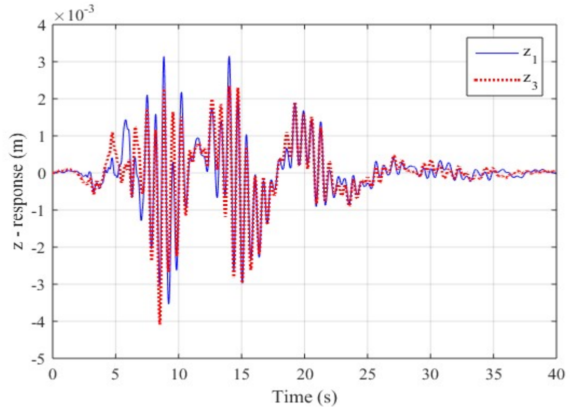

Fig. 15(b) Horizontal nodal response

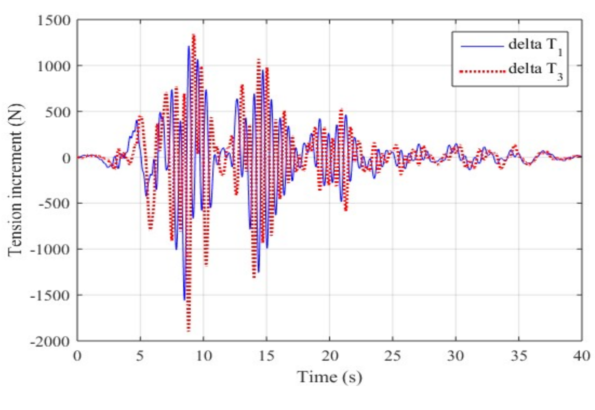

Fig. 16(a) Tension increment of inclined cable segments

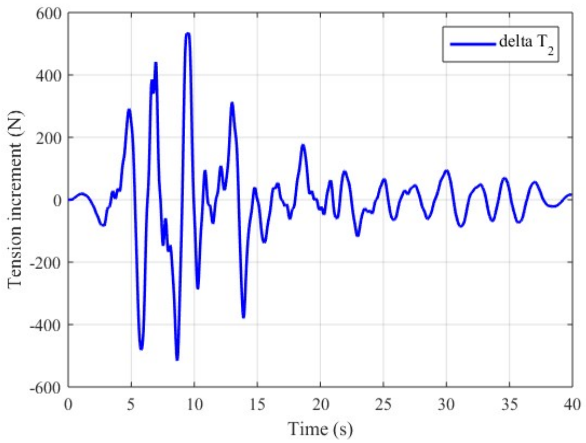

Fig. 16(b) Tension increment of horizontal cable segments

6. Discussion

In this paper the seismic response of sagging elasto-flexible cable is investigated with two distinct seismic excitation available named El Centro (1940) and Loma Prieta (1989). The author earlier investigated the same problem by adopting Force Model and find interesting results of sagging cable vibration [13]. The earthquake excitation is applied to the cable structure in three different ways. In first case, only horizontal seismic force is applied while in the second case only vertical seismic forces is applied. In third case both horizontal as well as vertical seismic force is applied simultaneously. It is important to note that, the vertical seismic force vector remains parallel to the sustained load vector. As the relative magnitudes of the sustained nodal forces remain same for the duration of the earthquakes, the vertical seismic force vector represents the proportionate load vector. On the other hand, the horizontal seismic force vector observed to remain orthogonal to the sustained load vector.

It is predicted that the tension increment response in the inclined cable segments are of similar order irrespective of the case of application of the seismic excitation. In other words the tension increments in the inclined cable segments due to seismic force are more or less same in all the cases of seismic force. This behaviour is shown by both El Centro and Loma Prieta ground excitation. This is due to the facts that the part or full inertia force is always taken by inclined cable segments.

The tension increment in the horizontal cable segment is negligible when only horizontal seismic force is applied whereas the tension increment in all the cable segments are same when only vertical seismic force is applied. This can be due to horizontal seismic excitation, relative change in horizontal inertial force is zero due to similar mass at the both node. This confirms the facts that due to horizontal seismic force horizontal nodal vibration are symmetric and hence no tension increments should be there.

It is very interesting to note that, when only vertical seismic forces is applied the maximum horizontal nodal response amplitude is negligible although the tension increment in the horizontal cable segment is of the order 1.2 kN. This is due to anti-symmetric vibration of the both node in horizontal direction.

7. Conclusion

The predicted seismic responses confirm the facts that the vertical vibration of the cable nodes is symmetric under vertical seismic force and anti-symmetric under horizontal seismic forces. Similarly the horizontal vibration of the cable nodes is symmetric under horizontal seismic forces and anti-symmetric under vertical seismic forces. The change in the tension in the inclined cable shows maximum variation in all the condition of application of the seismic excitation. The horizontal cable segment shows maximum tension variation in case of anti-symmetric nodal vibration in horizontal direction, whereas minimum or negligible variation in case of symmetric horizontal nodal vibration. The present investigation shows interesting facts about the nonlinear characteristics of the cable vibration with simple approach. The investigation may help to understand the basic dynamics of the sagging cable.

Acknowledgement

The authors express their sincere thanks towards the National Project Implementation Unit (NPIU) MHRD, New Delhi, India for providing research grant for this work.

References

1. Irvine, H.M. and Caughey, T.K. The linear theory of free vibrations of a suspended cable. Mathematical and Physical Sciences, 1974; 341(1626): 299-315.
2. Lacarbonara, W., Paolone, A. and Vestroni, F. Non-linear modal properties of non-shallow cables. Int. J. of Non-Linear Mechanics, 2007; 42: 542-554.
3. Fried, I. Large deformation static and dynamic finite element analysis of extensible cables, Computers and Structures, 1982; 15(3): 315-319.
4. Koh, C.G, Zhang, Y. and Quek, S.T. Low-tensioned cable dynamics: numerical and experimental Studies. 1999; J. of Eng. Mechanics, 125(3): 347-354.
5. Thai, H.T. and Kim, S.E. Nonlinear static and dynamic analysis of cable structures, Finite Elements in Analysis and Design, 2011; 47: 237-246.
6. Volokh, K.Y., Vilnay, O. and Averbuh, I. Dynamics of cable structures. Journal of Engineering Mechanics, 2003; 129(2): 175-180.
7. Kamel, M.M. and Hamed, Y.S. Nonlinear analysis of an elastic cable under harmonic excitation.” Acta Mech. Springer-Verlag., 2010; 214: 135-325.
8. Kumar P., Ganguli A. and Benipal G.S. Theory of weightless sagging elasto-flexible cables. Latin American Journal of Solids and Structures, 2016; 13(1): 155-174.
9. Kumar P., Ganguli A. and Benipal G.S. Comparative assessment of the contending force and placement methods for weightless sagging cables. Asian Journal of Civil Engineering, 2019; 20(7): 1049-1062.

10. Clemente, P., Celebi, M., Bongiovanni, G., and Rinaldis, D. Seismic analysis of the Indiano cable-stayed bridge. In 13th World Conference on Earthquake Engineering, Vancouver, BC, Canadá, 2004. paper (No. 3296).

11. Gong, Jun, Xudong Zhi, Feng Fan and Shizhao Shen. Static and dynamic stiffness in the modeling of inclined suspended cables. Journal of Constructional Steel Research 172 (2020), pp. 106210.

12. Tian, Li, and Xia Gai. Nonlinear seismic behavior of different boundary conditions of transmission line systems under earthquake loading. Shock and Vibration (2016).

13. Kumar, P., Ganguli, A., and Benipal, G.S. Seismic analysis of weightless sagging elasto-flexible cables. In Advances in Structural Engineering, Springer, New Delhi, 2015; 1543-1562.